Journal of Zhejiang University-SCIENCE A (Applied Physics & Engineering) *2023 24(11):949-959*
www.jzus.zju.edu.cn; www.springer.com/journal/11582
E-mail: jzus_a@zju.edu.cn

Research Article

https://doi.org/10.1631/jzus.A2200468

Effect of carbon dioxide concentration on the combustion characteristics of boron agglomerates in oxygen-containing atmospheres

Lian DUAN, Zhixun XIA, Yunchao FENG, Binbin CHEN✉, Jiarui ZHANG, Likun MA

College of Aerospace Science and Engineering, National University of Defense Technology, Changsha 410073, China

Abstract: In ramjet combustion chambers, carbon dioxide (CO_2) produced by the combustion of carbonaceous fuel enters the chamber together with boron agglomerates. In order to investigate the effect of CO_2 concentration present in an oxygen-containing atmosphere on the combustion characteristics and oxidation mechanisms of boron agglomerates, we used a laser ignition system, an X-ray diffractometer (XRD), and a thermogravimetric-differential scanning calorimetry (TG-DSC) combined thermal analysis system. Single-particle boron was tested in the laser-ignition experiments as the control group. The ignition experiment results showed that with a fixed O_2 concentration of 20%, when the particle temperature reaches the melting point of boron, increasing CO_2 content causes the combustion process of boron agglomerates to transition from single-particle molten droplet combustion to porous-particle combustion. Furthermore, XRD analysis results indicated that the condensed-phase combustion products (CCPs) of boron particles in a mixed atmosphere of O_2 and CO_2 contained B_4C, which is responsible for the porous structure of the particles. At temperatures below 1200 °C, the addition of CO_2 has no obvious promotion effect on boron exothermic reaction. However, in the laser-ignition experiment, when the oxygen concentration was fixed at 20% while the CO_2 concentration increased from 0% to 80%, the maximum temperature of boron agglomerates rose from 2434 to 2573 K, the self-sustaining combustion time of single-particle boron decreased from 396 to 169 ms, and the self-sustaining combustion time of boron agglomerates decreased from 198 to 40 ms. This study conclusively showed that adding CO_2 to an oxygen-containing atmosphere facilitates boron reaction and consumption pathways, which is beneficial to promoting exothermic reaction of boron agglomerates at relatively high temperatures.

Key words: Boron combustion; Amorphous boron; Boron-containing propellant; Solid fuel ramjet

1 Introduction

Boron is regarded as an ideal energetic additive for solid propellants because of its high volumetric and gravimetric heating values (Fry, 2004), so it is widely used in solid-fuel ramjets and scramjets (Lv et al., 2017; Chen et al., 2018; Zhang et al., 2020). In a ramjet gas generator, boron particles are likely to agglomerate into large particles due to low melting point and high viscosity of the oxide layer on the surface of boron particles (Meerov et al., 2015; Liu et al., 2017). The combustion of the carbonaceous formulation in a boron-based fuel-rich propellant produces a large amount of CO_2 (Liu et al., 2015), which affects the combustion characteristics of boron agglomerates. In addition, direct combustion heating is often used in ramjet ground simulation tests, to increase the air temperature during simulation of the total temperatures of air flows entering the secondary combustion chamber in flight state (Roux et al., 2014). When the working medium of the heater uses an air/alcohol or air/kerosene mixture, the level of CO_2 in the air entering the combustion chamber exceeds 10% (Li et al., 2007).

Researchers have performed a considerable amount of work on the effects of fluorine-containing atmosphere (Krier et al., 1996; Zhou et al., 1998; Ulas et al., 2001) and water vapor (Smolanoff et al., 1996; Foelsche et al., 1999; Yoshida and Yuasa, 2000) on the ignition and combustion characteristics of boron particles, and improved the understanding of the energy-release characteristics of such particles. However, few studies have addressed the ignition and combustion characteristics of boron in a CO_2-containing atmosphere. Experiments conducted by DiGiuseppe and Davidovits

✉ Binbin CHEN, chenbinbin11@nudt.edu.cn
Lian DUAN, https://orcid.org/0009-0009-9836-9714

Received Oct. 4, 2022; Revision accepted Feb. 22, 2023;
Crosschecked Aug. 7, 2023

(1981) revealed that the reaction between boron and CO_2 produced BO and CO, with an exothermic heat of (67±5) kcal/mol (1 kcal=4.186 kJ) and a relatively slow reaction rate. Burkholder et al. (1993) conducted a condensation reaction of pulsed laser-evaporated boron atoms with CO_2 in excess Ar, and infrared spectrum analysis of the reaction products showed that OBCO was generated in addition to BO and CO. Thus, they concluded that OBCO was the main product of the reaction between boron and CO_2. Chin et al. (2003) calculated the reaction between B and CO_2 by ab initio and density functional methods, and found that the reaction first generated a dynamically unstable intermediate, BOCO, which then decomposed into BO and CO, and finally formed the most stable thermodynamic substance: OBCO. Li et al. (2014) analyzed the effect of CO_2 concentration on the thermal oxidation characteristics of boron particles by thermogravimetry, and found that appropriate concentrations of CO_2 (10% or 30%) in a limiting O_2 (10%) atmosphere facilitated the onset of oxidation of boron particles and improved ignition performance.

A CO_2 atmosphere can affect the thermal oxidation characteristics of boron particles, but the specific reasons for this effect are yet to be elucidated. Especially about the effects of boron agglomerates, little is known. In this study, we directly observed the structural and morphological evolution of boron agglomerates during combustion, and analyzed the combustion process and spectral data. The temperature evolution of the particle surface was obtained through a fitting procedure using the Planck law. The microscopic morphology and rough elemental composition of condensed-phase combustion products (CCPs) were analyzed with a scanning electron microscope (SEM) and energy dispersive spectrometer (EDS), and the phase-crystal structures were analyzed by X-ray diffractometer (XRD). Additionally, we employed thermogravimetric-differential scanning calorimetry (TG-DSC) to study the oxidation process. The results of this study provide a reference for the energy-release mechanism of boron agglomerates when O_2 and CO_2 coexist.

2 Experimental procedures

2.1 Materials

We carried out our comparative experiments on amorphous boron agglomerates and single-particle crystalline boron. The boron agglomerates were prepared by drying a slurry of the micron-sized amorphous boron in water (Mi et al., 2013). The initial amorphous boron was available commercially from Yingkou Liaobin Fine Chemicals Co., Ltd., China, with a purity of 96% and mean diameter of 2.55 μm. The agglomerate density was measured by the Archimedes drainage method to be 1.27 g/cm^3. The single-particle crystalline boron was obtained from Zhongnuo Advanced Material Technology Co., Ltd., China, with a purity of 99.9%. The boron agglomerates and single-particle boron between 355 and 400 μm were screened by a sieve shaker. The samples used in the test are shown in Fig. 1.

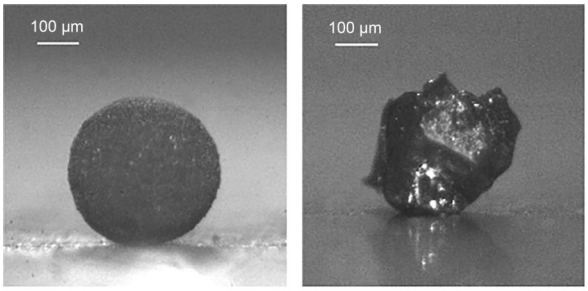

Fig. 1 Amorphous boron agglomerate (a) and single-particle crystalline boron (b)

2.2 Apparatus and methods

A laser-ignition test system was used to investigate the effect of CO_2 concentration on the combustion characteristics of boron agglomerates in oxygen-containing atmospheres. A schematic diagram of the experimental setup is given in Fig. 2. The same system was successfully used in an earlier ignition study on boron agglomerates (Duan et al., 2022). All combustion tests were conducted under constant laser power and laser duration, and the laser loading time was set to 250 ms. We measured the actual power emitted to the sample surface in different atmospheres with a power meter (F150A-BB-26, Ophir, Israel) as (85.0±0.3) W.

A monochrome high-speed camera (Dimax HS4, PCO, Germany), a color high-speed camera (FASTCAM SA-X2, Photron, Japan), and a fiber-optic spectrometer (HR2000+ES, Oceanoptics, USA) were employed to monitor the combustion process of the sample through high-purity quartz-glass windows. Flame images were photographed using the color high-speed camera, with an exposure time of 200 μs and a frame

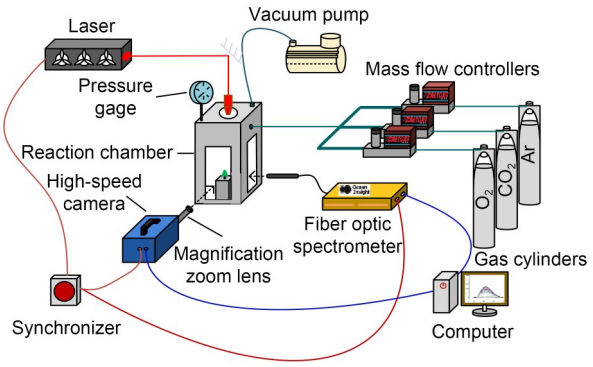

Fig. 2 Schematic diagram of the laser-ignition experimental system

rate of 5000 frame/s, while the particle-surface morphology evolution was recorded with the monochrome high-speed camera, with an exposure time of 900 μs and a frame rate of 1000 frame/s. The fiber spectrometer measured the spectrum within the wavelength range of 200–1100 nm, while the integration time was fixed at 1 ms. Before each experiment, the spectrometer recorded the background radiation spectrum. During the experiment, the data collected by the spectrometer automatically deducted the background radiation spectrum.

In all ignition tests, the burner pressure was kept at 1.013×10^5 Pa, the total gas-flow rate was precisely controlled by a mass flowmeter to be constant at 10 mL/min, the flow rate of O_2 was fixed at 2 mL/min, and the flow ratios of Ar and CO_2 were varied to set the concentrations of CO_2 in the burner as 0%, 20%, 40%, 60%, or 80%. In addition, the operating conditions of a pure CO_2 atmosphere were set as the control. At least 10 repetitive experiments were performed under each condition to ensure the reliability of the experimental results.

After the ignition test, we analyzed the microscopic morphology and rough elemental composition of the CCPs with an SEM (JEOL, JSM-7900F, Japan) combined with EDS. The phase crystal structures of CCPs were analyzed with an XRD instrument (D8 Advance, Bruker, Germany).

For thermo-analytical measurements, we used a Netzsch STA 449F3 simultaneous thermal analyzer. A total of 8.5–10.0 mg boron agglomerates were packed in alumina crucibles. Three flowmeters controlled the total flow rate into the furnace of the analyzer to be 100 mL/min, and different atmospheres were obtained by changing the flow ratios of O_2, CO_2, and Ar. The test atmospheres were set to 20% O_2+80% Ar, 20% O_2+40% CO_2+40% Ar, 20% O_2+80% CO_2, and pure CO_2. A well-proportioned gas flow was continuously fed into the furnace for 10 min before each programmed temperature rise to ensure that the gas environment was well controlled. In addition, the test data of an empty crucible in various atmospheres were obtained for baseline correction.

3 Results and discussion

3.1 Surface-morphology analysis

Figs. 3a–3c illustrate the temporal evolution of the surface morphology of boron agglomerates when the oxygen concentrations were kept at 20% while the CO_2 concentration was 0%, 40%, and 80%, respectively. The image parameters such as contrast, brightness, and other settings were the same. We recorded the moment when the laser started to radiate to the particle as 0 ms. It can be seen from Fig. 3a that, in the oxygen-containing atmosphere without CO_2, the particles gradually melted into a liquid state. After 250 ms, the laser stopped loading, and the particles underwent self-sustained combustion for a while. This was similar to the process observed in our previous study (Duan et al., 2022). As can be seen from Fig. 3b, in the oxygen-containing atmosphere with 40% CO_2 concentration, no melting trace of particles could be observed in the first 150 ms of laser loading. At 200 ms, partial reflection appeared on the particle surface, and it changed into a semi-molten state at 250 ms.

Fig. 3c shows that in the oxygen-containing atmosphere with 80% CO_2 concentration, the particle-combustion process did not exhibit a melting state,

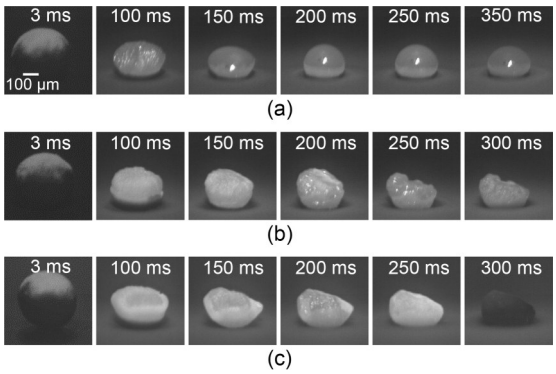

Fig. 3 Surface morphologies of boron agglomerates with different CO_2 concentrations: (a) 20% O_2+80% Ar; (b) 20% O_2+40% CO_2+40% Ar; (c) 20% O_2+80% CO_2

and there was no obvious liquid film covering the particle surface. The upper surface of the particle collapsed downward and the surface morphology was irregular. At 300 ms, the particles had cooled and the surface had dimmed. Comparing the images shown in Figs. 3a–3c, we found that with a fixed oxygen concentration of 20%, the higher the CO_2 concentration, the lower the melting degree of the particles, the more irregular the particle morphology, and the faster the particle-cooling rate after the laser had stopped loading.

The light source was placed opposite to the camera as a background light so that we could observe the morphological changes in the particle profile during combustion. Figs. 4a and 4b show the combustion processes of single-particle crystalline boron in atmospheres of 20% O_2+80% Ar and 20% O_2+80% CO_2, respectively. As seen from Fig. 4a, in the mixed atmosphere of oxygen and argon, the contour lines of single-particle boron gradually became smooth, and the particles gradually melted into a hemispherical shape. Fig. 4b shows that in the oxygen-containing atmosphere with 80% CO_2 concentration, the smoke overflowed from the particle surface to the environment at about 50 ms, and a large amount of smoke was generated around the crystalline boron particles during the subsequent combustion process. After flameout, the thickness of deposition products accumulated around the particles was greater.

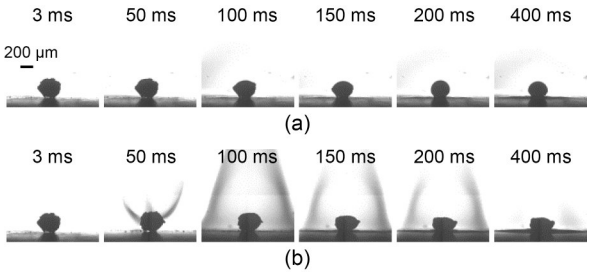

Fig. 4 Particle-profile evolution of single-particle boron: (a) 20% O_2+80% Ar; (b) 20% O_2+80% CO_2

3.2 Analysis of the combustion process

The ignition and combustion processes of boron agglomerates in atmospheres with different CO_2 concentrations are illustrated in Fig. 5. The time of laser initiation (0 ms) was used as the reference time. After laser loading, a faint green flame appeared above the particles in both the 20% O_2+80% Ar atmosphere and 20% O_2+80% CO_2 atmosphere, caused by light emission

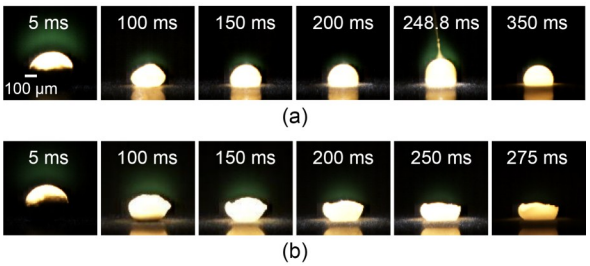

Fig. 5 Combustion process of boron agglomerates in different atmospheres: (a) 20% O_2+80% Ar; (b) 20% O_2+80% CO_2. References to color refer to the online version of this article

from the gaseous intermediate BO_2 (Yuasa and Isoda, 1991).

Comparing Figs. 5a and 5b, it becomes clear that in the 20% O_2+80% Ar atmosphere, there was an ejection phenomenon during the combustion process of boron agglomerates, as shown in Fig. 5a at 248.8 ms. However, the boron agglomerates did not melt into a hemispherical shape in an atmosphere of 20% O_2+80% CO_2, and the upper surface of the particles was highly irregular during combustion. We speculated that this was due to the reaction of boron and CO_2 generating other substances in the CO_2-rich atmosphere, which did not melt easily or suppressed the exotherm of the reaction system. After 250 ms, the laser stopped loading, and the particles were in self-sustained combustion for a while. Then, the reaction rate gradually decreased and the flame was extinguished. Fig. 5 shows that the flameout rate was faster in an atmosphere containing CO_2.

3.3 Combustion-spectrum analysis

Fig. 6 illustrates the combustion spectra of boron agglomerates at the moment of maximum spectral intensity in a pure CO_2 atmosphere, pure Ar atmosphere, and 20% O_2+80% CO_2 atmosphere. During the combustion process of boron agglomerates in the oxygen-containing atmosphere, the spectral signals of gas-phase intermediates BO and BO_2 were emitted, causing the wavelength curves to contain multiple distinct characteristic peaks (Yoshida and Yuasa, 2000; Song et al., 2021). In a pure CO_2 atmosphere, there were no emission peaks for BO and BO_2 in the spectral curve, indicating that the reaction between boron and CO_2 did not produce the gas-phase intermediate products BO and BO_2. In a pure Ar atmosphere, the particle temperature was raised by laser radiation, and spectral fluctuation was

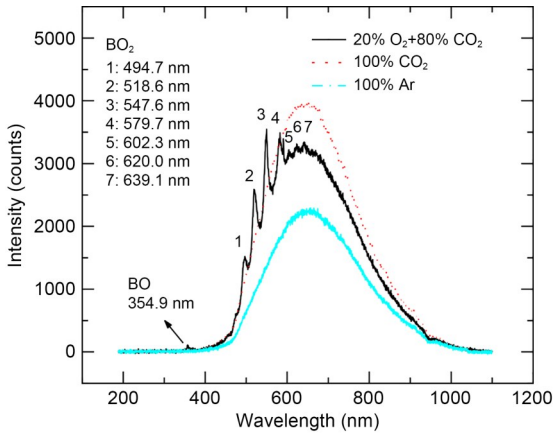

Fig. 6 Combustion spectra with the maximum intensity for boron agglomerates in different atmospheres

detected by the spectrometer. However, the spectral intensity was relatively low because boron particles did not undergo exothermic reaction in the Ar atmosphere.

Both the ignition and combustion processes of boron particles in the oxygen-containing atmosphere emitted the spectral signal of BO_2, and the strongest spectrum intensity corresponded to a wavelength of 547.6 nm. Fig. 7 shows that after laser loading, the spectral intensity signals increased rapidly for atmospheres of 20% O_2+80% CO_2 and 20% O_2+80% Ar, and then decreased slowly, due to the surface reaction and phase transition during the combustion process changing the emissivity of the particle surface, as well as the solidified B_2O_3 around the particle absorbing some of the radiation (Yuasa and Isoda, 1991; Millot et al., 2002). Curve B has two troughs at about 50 and 190 ms, which may be related to other substances produced by the reaction of boron and CO_2. After the laser has been

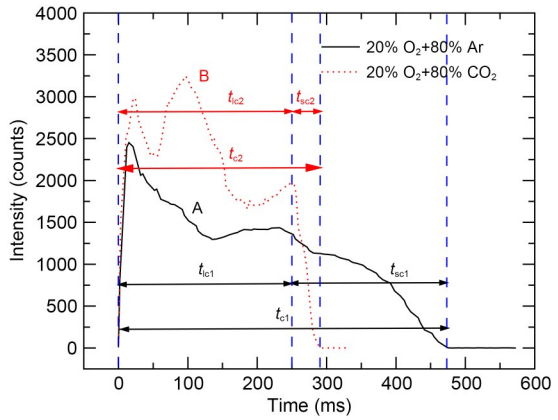

Fig. 7 Temporal variation of spectral intensity at a wavelength of 547.6 nm

continuously loaded for 250 ms and then deactivated, the spectral intensity of curve B dropped sharply.

The duration of availability of the 547.6 nm spectral signal was defined as the combustion time (Song et al., 2021). The laser turn-on time was recorded as 0 ms. The combustion time (t_c) can be further divided into combustion time with laser loading (t_{lc}) and self-sustaining combustion time after laser loading (t_{sc}). Under these experimental conditions, the longer the particle-combustion time, the slower the decrease in chemical reaction rate after laser deactivation, and thus the self-sustaining combustion lasted longer.

Fig. 8 shows the self-sustaining combustion time of single-particle crystalline boron and amorphous boron agglomerates at different CO_2 concentrations when the oxygen concentration was 20%. The self-sustained combustion time of both single-particle boron and boron agglomerates decreased significantly with increasing CO_2 concentration. When the CO_2 concentration was increased from 0% to 80%, the self-sustaining combustion time of boron agglomerates decreased from 198 to 41 ms, and that of single-particle boron decreased from 397 to 170 ms. The higher the CO_2 concentration, the faster the chemical reaction rate decreased, and therefore the shorter the self-sustaining combustion time became. This suggests that when boron is burned in an oxygen-containing atmosphere, the higher the CO_2 concentration, the more sensitive the chemical reaction rate is to the temperature changes.

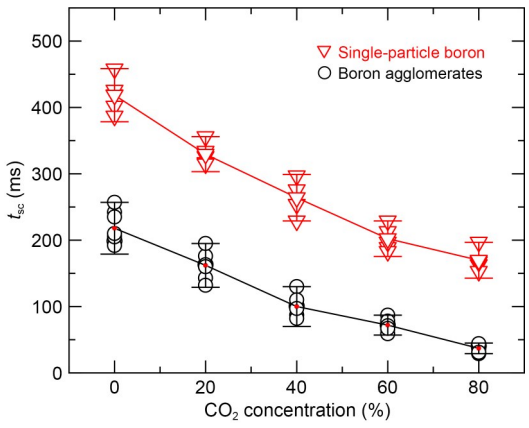

Fig. 8 Self-sustaining combustion time of single-particle boron and boron agglomerates with different CO_2 concentrations

3.4 Temperature analysis

The temperature evolution of the particle surface was obtained through a fitting procedure using the

Planck law (Mi et al., 2013). The calculation method and error analysis are illustrated in the electronic supplementary materials (ESM).

Fig. 9 shows the temporal variation in particle temperature when the oxygen concentration was fixed at 20% and the CO_2 concentrations were 0%, 40%, and 80%. The time interval of temperature data was 10 ms. After laser activation, the particle temperature in all three atmospheres rapidly increased to above the boiling point of B_2O_3 (2316 K), so the boron oxide layer on the particle surface could be quickly removed by evaporation. Within 250 ms of laser loading, when the CO_2 concentration was increased from 0% to 80%, the maximum surface temperature of the boron agglomerates rose from 2434 to 2573 K, which is between the melting points of boron (2350 K) and B_4C (2623 K). After 250 ms, the particle temperature in the 20% O_2+80% CO_2 atmosphere decreased rapidly, while in the 20% O_2+80% Ar atmosphere, the high temperature was maintained for a period.

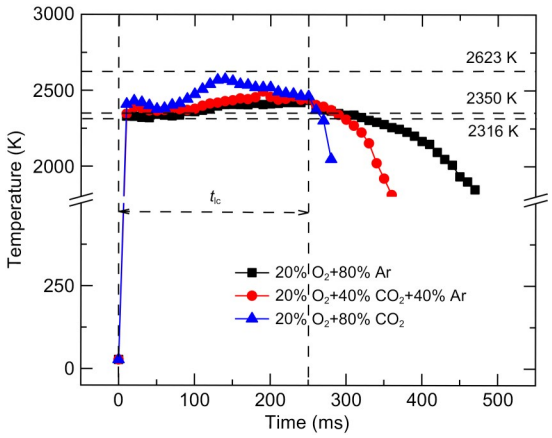

Fig. 9 Temperature variation of the boron agglomerates with different CO_2 concentrations

3.5 Analysis of condensed combustion products

It is helpful to explore the combustion process of boron agglomerates in typical atmospheres by analyzing the residual CCPs after particle flameout. Field emission scanning electron microscope (FE-SEM) images of the CCPs of amorphous boron agglomerates in the 20% O_2+80% CO_2 atmosphere, as well as single-particle crystalline boron in the 20% O_2+80% CO_2 atmosphere, are shown in Figs. 10a and 10b, respectively. Fig. 10a shows that the structure was curly and the surface morphology was very rough; they lost their initial granular structure and contained a large number of pores with obvious wrinkles. The rough surface increased the contact area between the oxidizing gas and the particle surface. The clear crystal structure was discernible by magnifying the particle surface. The surface of CCPs of single-particle boron lost its initial flat morphology and also became rough, with an obvious crystal structure (Fig. 10b). We have previously observed the microscopic morphology of the CCPs of boron agglomerates

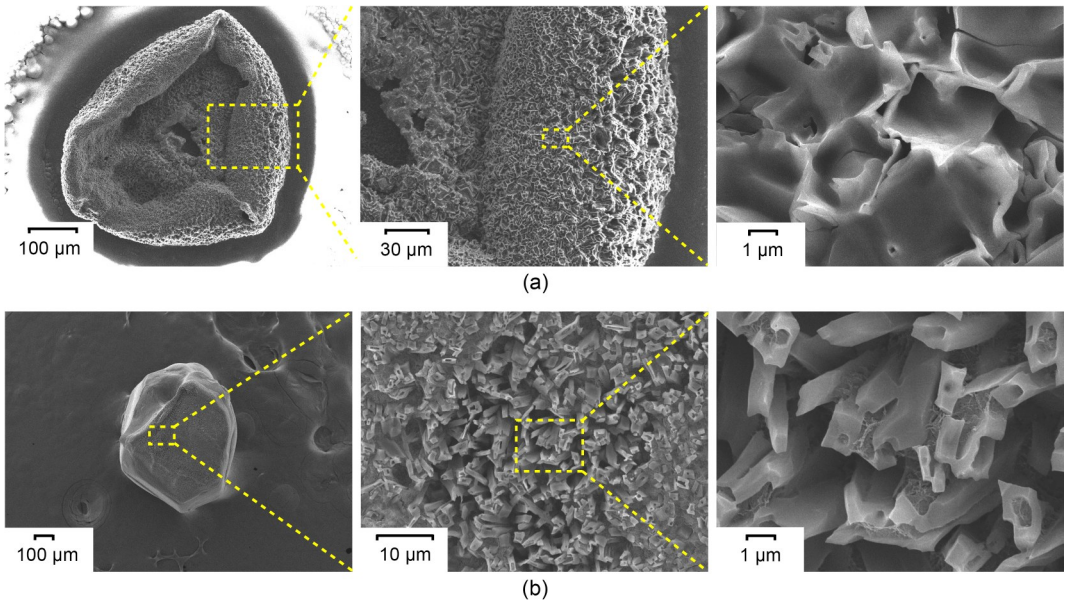

Fig. 10 FE-SEM images of CCPs: (a) CCP of boron agglomerate in 20% O_2+80% CO_2 atmosphere; (b) CCP of single-particle boron in 20% O_2+80% CO_2 atmosphere

in pure oxygen and mixed atmospheres of oxygen and argon (Duan et al., 2022), and found that there were no wrinkles or similar crystal structures on the particle surface, which is significantly different from the morphologies observed here.

Subsequently, we analyzed the micro-area elementary composition of the CCPs of single-particle crystalline boron in an atmosphere of 20% O_2+80% CO_2. The results of this analysis are shown in Fig. 11. We observed that the distribution of C was dense in the wrinkled regions, while the distribution of O was dense in the smooth regions. Elemental composition analysis of the wrinkled regions in Figs. 10a and 10b revealed that the predominant elements were B and C.

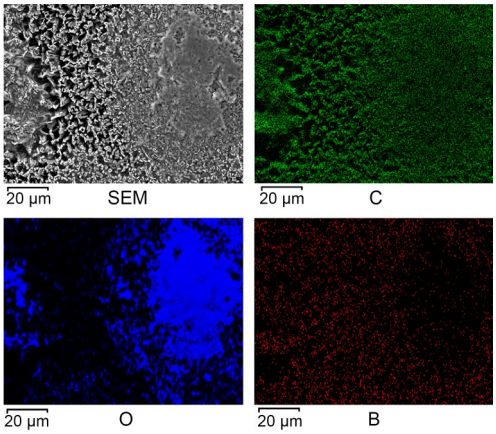

Fig. 11 Reference image of SEM and EDS elemental maps corresponding to elements C (green points), O (blue points), and B (red points). References to color refer to the online version of this figure

To explore the crystal structures formed by the reaction of boron and CO_2 in oxygen-containing atmospheres, we placed the compacted amorphous boron stack in an atmosphere with an oxygen concentration of 20% and a CO_2 concentration of 80%, for laser ignition. The power level and duration of the laser were consistent with the above ignition experiments. Then, the CCPs were taken for XRD analysis. The obtained XRD pattern is shown in Fig. 12. The intense peaks at around 2θ=20°, 22°, 23°, 35°, and 38° corresponded to boron carbide (B_4C) (Jain and Anthonysamy, 2015), indicating that boron can react with CO_2 to form B_4C in an oxygen-containing atmosphere. Additionally, peaks for B_2O_3 were identified at around 2θ=14° and 28° (Hashim et al., 2021), while few low-intensity crystal boron peaks were observed due to the incomplete reaction of the tested sample (Sun et al., 2018).

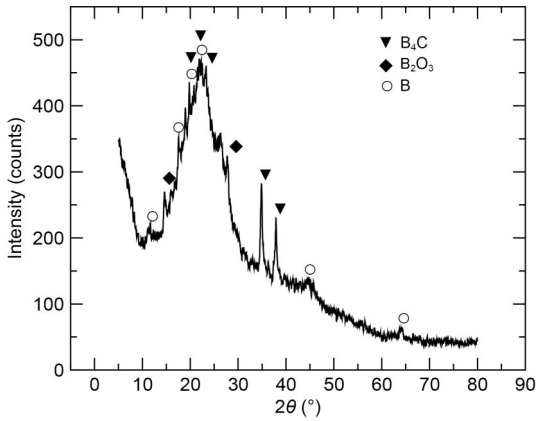

Fig. 12 XRD pattern of CCPs in 20% O_2+80% CO_2 atmosphere

3.6 Low-temperature exothermic reaction

TG and DSC traces for amorphous boron in 20% O_2+80% Ar, 20% O_2+40% CO_2+40% Ar, 20% O_2+80% CO_2, and pure CO_2 atmospheres at a heating rate of 20 °C/min are shown in Fig. 13.

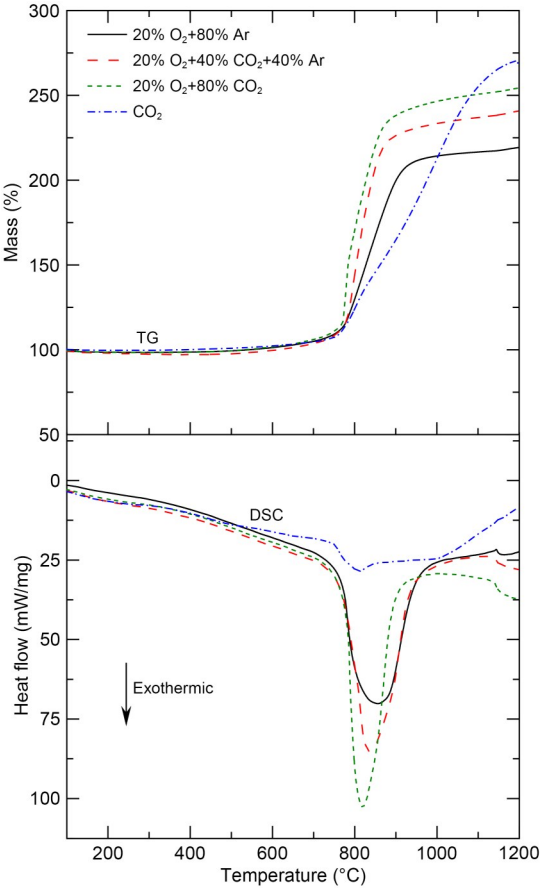

Fig. 13 TG and DSC traces of amorphous boron in different atmospheres heated at 20 °C/min to a maximum temperature of 1200 °C

Oxidation of boron began at around 550 °C in all atmospheres. In an atmosphere with a fixed oxygen concentration of 20%, the oxidation rate increased with the increase of CO_2 content after reaching approximately 750 °C. We speculate that after the oxide layer on the outer surface of the boron particles melts, O_2 and CO_2 diffuse simultaneously through the liquid oxide layer and react with the boron core. Therefore, the higher the CO_2 content, the greater the mass gain of the sample and the more advanced the exothermic peak. At temperatures above 850 °C, the mass gain of the boron particles tended to be gentle. This is likely due to the accumulation of reaction products on the particle surface, which thickens the liquid oxide layer and inhibits the reaction between the gases and the boron core.

In an atmosphere of pure CO_2, the oxidation process continued and eventually surpassed the mass gain of boron in O_2-CO_2 mixtures. However, the heat release was comparatively low. This is most likely because boron reacts with CO_2 to form BOCO during this period, with an exothermic heat of about 25 kcal/mol (Chin et al., 2003), which is far lower than the exothermic heat of 146 kcal/mol of the reaction between boron and oxygen (King, 1973).

3.7 Discussion

The above experimental results demonstrated that B_4C in a ramjet combustion chamber can form not only by the reaction of boron with hydrocarbons generated by the decomposition of carbon-based compounds (such as hydroxyl terminated polybutadiene in propellant (Liu et al., 2015)) but also by the reaction of boron with atmospheric CO_2 at high temperature. B_4C can further react with oxygen to form the thermodynamically stable compound B_2O_3 (Jain and Anthonysamy, 2015). B_2O_3 is the main product of B_4C combustion (Li and Qiu, 2007), and the relevant reaction is expressed by Eq. (1). During the continuous loading of the laser, the surface temperature of particles was higher than the boiling point of B_2O_3 (2316 K), and the B_2O_3 evaporated from the surface and condensed around the particles to form obvious smoke, as shown in Fig. 4b. Our conjecture is that at high temperature, CO_2 in an oxygen-containing atmosphere increases the combustion efficiency of boron particles, due to the continuous generation and consumption of B_4C.

$$B_4C + 4O_2 \rightarrow CO_2 + 2B_2O_3. \quad (1)$$

The calorific value of B_4C is 52 MJ/kg, which is similar to that of boron (59 MJ/kg). However, the melting point of B_4C is about 300 K higher than that of boron; hence, it will be relatively difficult to melt into liquid phase. The temperature in this experiment reached the melting point of boron but not that of B_4C. The latter adhered to molten boron and changed the physicochemical properties and combustion state of the particles.

Based on the above analysis, a schematic diagram of the structural evolution of boron agglomerates during combustion is shown in Fig. 14. When the agglomerated boron is heated, individual boron particles tend to bond together due to the low melting point and high surface tension of their oxide layer, resulting in the volume of the agglomerate shrinking, as shown in Fig. 14b. At a fixed O_2 concentration of 20%, as the CO_2 concentration increased from 0% to 80%, the maximum surface temperature of the boron agglomerates rose from 2434 to 2573 K, which was between the melting points of B and B_4C. In an atmosphere with

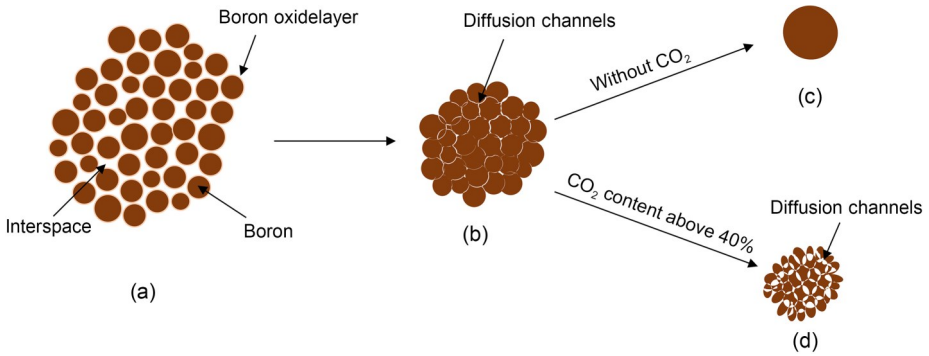

Fig. 14 Schematic of the internal structural evolution of boron agglomerates during heating and combustion in atmospheres with different CO_2 concentrations: (a) original boron agglomerate; (b) shrunken agglomerate; (c) molten droplet; (d) porous particle

low or no CO_2 content, after the agglomerate's temperature reaches the melting point of boron, it gradually melts into droplets, as shown in Fig. 14c. These droplets lose their original agglomeration morphology, and the oxidizing gases cannot diffuse inside through the pores. Droplets with larger particle sizes tend to have longer combustion times in practical application, resulting in incomplete combustion (Sun et al., 2020). In an atmosphere with a CO_2 content of more than 40%, the amount of boron carbide produced is greater than the amount consumed by its reaction with oxygen, causing it to dominate the agglomerate and further transforming it into a porous structure, as shown in Fig. 14d. Gases such as O_2 and CO_2 can diffuse into the interior of the agglomerate through the pores, leading to an accelerated rate of boron consumption. When the CO_2 concentration is between 20% and 40%, the agglomerate structure is in a semi-molten state during combustion, and the local area of the particle surface may be rough due to the reaction with CO_2.

After the laser stopped radiation heating, we noted that the higher the concentration of CO_2 became, the shorter the self-sustaining combustion time of single-particle boron and boron agglomerates was. With a fixed oxygen concentration of 20%, when CO_2 concentration was increased from 0% to 80%, the self-sustaining combustion time of single-particle boron decreased from 396 to 169 ms, and that of boron agglomerates decreased from 198 to 40 ms. Therefore, it seems that the higher the CO_2 concentration, the greater the content of generated B_4C, and the higher the content of B_2O_3 generated by the reaction between B_4C and oxygen. After the laser stopped loading, in the absence of continuous heating from any external heat source, the temperature gradually decreased. When the particle surface temperature was lower than the boiling point of B_2O_3 (2316 K), B_2O_3 generated by surface reaction accumulated on the surface of B_4C, forming a glassy liquid film that acted as a barrier to the further diffusion of oxygen into B_4C and to the release of CO_2 from B_4C (Li and Qiu, 2007), such that the reaction rate decreased rapidly and the flame was quickly extinguished. In the atmosphere without CO_2, the self-sustaining combustion time of particles was longer. This is because the B_2O_3 produced by the reaction of boron and oxygen was formed by further oxidation of the intermediate products in the gas phase (Burkholder and Andrews, 1991; Zhou, 1998). The relevant reaction pathway is presented in Eqs. (2)–(4) (Burkholder and Andrews, 1991; Liang et al., 2017). Therefore, when the particle temperature drops below the boiling point of boron oxide, the B_2O_3 in the environment will not completely diffuse and cover the particle surface, and the particle surface can still be in direct contact with oxygen in the environment for an exothermic reaction, thereby self-sustaining combustion for a relatively long time.

$$\mathrm{B(l)+O_2(g)\rightarrow BO(g)+O(g)}, \tag{2}$$

$$\mathrm{BO(g)+O_2(g)\rightarrow BO_2(g)+O(g)}, \tag{3}$$

$$\mathrm{BO_2(g)+BO(g)\rightarrow B_2O_3(g)}. \tag{4}$$

To the best of our knowledge, the mechanism model of boron ignition and combustion established by Yetter et al. (1991), Zhou (1998), and Zhou et al. (1999), based on the detailed reaction mechanism and molecular dynamics theory, did not consider the reaction process after boron reacts with CO_2 to generate CO and BO. Therefore, the path and thermodynamic parameters of the reaction on the particle surface that generates B_4C need to be further explored.

4 Conclusions

In this work, we investigated the effect of CO_2 concentration on the combustion characteristics of amorphous boron agglomerates by changing the flow ratios of CO_2 to Ar while maintaining a constant oxygen concentration of 20%. The main findings are summarized as follows:

1. Boron agglomerates can react with CO_2 in an oxygen-containing atmosphere at high temperature to form B_4C, which increases the reaction and consumption pathways of boron and changes the physicochemical properties and combustion state of particles. With a fixed oxygen concentration of 20%, when particle temperatures reach the melting point of boron, an increase in CO_2 content causes the combustion process of boron agglomerates to transition from single-particle molten droplet combustion to porous-particle combustion.

2. At temperatures below 1200 °C, the addition of CO_2 has no obvious promotion effect on a boron exothermic reaction. However, in the laser ignition experiment, the maximum surface temperature of boron

agglomerates increased from 2434 to 2573 K when the oxygen concentration was fixed at 20% and the CO_2 concentration increased from 0% to 80%. Therefore, adding CO_2 to an oxygen-containing atmosphere is beneficial to promoting the exothermic reaction of boron agglomerates at relatively high temperatures.

3. With a fixed oxygen concentration of 20%, when the CO_2 concentration was increased from 0% to 80%, the self-sustaining combustion time of single-particle boron decreased from 396 to 169 ms, and that of boron agglomerates decreased from 198 to 40 ms. The higher the CO_2 concentration, the more quickly the chemical reaction rate decreases, and therefore the shorter the self-sustaining combustion time will be. This is presumably due to the fact that when the particle temperature is lower than the boiling point of B_2O_3, B_2O_3 produced by B_4C oxidation forms a glassy liquid film that covers the particle surface and acts as a barrier to hinder the further combustion of particles.

Acknowledgments

This work is supported by the National Natural Science Foundation of China (No. 52006240) and the Hunan Provincial Natural Science Foundation of China (Nos. 2020JJ4665 and 2021JJ30775).

Author contributions

Lian DUAN designed the research and wrote the first draft of the manuscript. Yunchao FENG and Binbin CHEN processed the corresponding data. Likun MA and Jiarui ZHANG helped to organize the manuscript. Zhixun XIA revised and edited the final version.

Conflict of interest

Lian DUAN, Zhixun XIA, Yunchao FENG, Binbin CHEN, Jiarui ZHANG, and Likun MA declare that they have no conflict of interest.

References

Burkholder TR, Andrews L, 1991. Reactions of boron atoms with molecular oxygen. Infrared spectra of BO, BO_2, B_2O_2, B_2O_3, and BO_2^- in solid argon. *The Journal of Chemical Physics*, 95(12):8697-8709. https://doi.org/10.1063/1.461814

Burkholder TR, Andrews L, Bartlett RJ, 1993. Reaction of boron atoms with carbon dioxide: matrix and ab initio calculated infrared spectra of OBCO. *The Journal of Physical Chemistry*, 97(14):3500-3503. https://doi.org/10.1021/j100116a010

Chen BB, Xia ZX, Huang LY, et al., 2018. Characteristics of the combustion chamber of a boron-based solid propellant ducted rocket with a chin-type inlet. *Aerospace Science and Technology*, 82-83:210-219. https://doi.org/10.1016/j.ast.2018.08.035

Chin CH, Mebel AM, Hwang DY, 2003. Theoretical study of the reaction mechanism of boron atom with carbon dioxide. *Chemical Physics Letters*, 375(5-6):670-675. https://doi.org/10.1016/S0009-2614(03)00964-3

DiGiuseppe TG, Davidovits P, 1981. Boron atom reactions. II. Rate constants with O_2, SO_2, CO_2, and N_2O. *The Journal of Chemical Physics*, 74(6):3287-3291. https://doi.org/10.1063/1.441534

Duan L, Xia ZX, Chen BB, et al., 2022. Ignition and combustion characteristics of boron agglomerates under different oxygen concentrations. *Acta Astronautica*, 197:81-90. https://doi.org/10.1016/j.actaastro.2022.05.020

Foelsche RO, Burton RL, Krier H, 1999. Boron particle ignition and combustion at 30–150 atm. *Combustion and Flame*, 117(1-2):32-58. https://doi.org/10.1016/S0010-2180(98)00080-7

Fry RS, 2004. A century of ramjet propulsion technology evolution. *Journal of Propulsion and Power*, 20(1):27-58. https://doi.org/10.2514/1.9178

Hashim SA, Islam M, Kangle SM, et al., 2021. Performance evaluation of boron/hydroxyl-terminated polybutadiene-based solid fuels containing activated charcoal. *Journal of Spacecraft and Rockets*, 58(2):363-374. https://doi.org/10.2514/1.A34820

Jain A, Anthonysamy S, 2015. Oxidation of boron carbide powder. *Journal of Thermal Analysis and Calorimetry*, 122(2):645-652. https://doi.org/10.1007/s10973-015-4818-3

King MK, 1973. Boron particle ignition in hot gas streams. *Combustion Science and Technology*, 8(5-6):255-273. https://doi.org/10.1080/00102207308946648

Krier H, Burton RL, Pirman SR, et al., 1996. Shock initiation of crystalline boron in oxygen and fluorine compounds. *Journal of Propulsion and Power*, 12(4):672-679. https://doi.org/10.2514/3.24088

Li HP, Ao W, Wang Y, et al., 2014. Effect of carbon dioxide on the reactivity of the oxidation of boron particles. *Propellants, Explosives, Pyrotechnics*, 39(4):617-623. https://doi.org/10.1002/prep.201300180

Li XP, Ge LH, Luan XT, 2007. Applications of gas generator in ramjet direct-connect test facility. *Journal of Rocket Propulsion*, 33(3):14-19 (in Chinese). https://doi.org/10.3969/j.issn.1672-9374.2007.03.003

Li YQ, Qiu T, 2007. Oxidation behaviour of boron carbide powder. *Materials Science and Engineering: A*, 444(1-2):184-191. https://doi.org/10.1016/j.msea.2006.08.068

Liang DL, Liu JZ, Zhou YN, et al., 2017. Ignition and combustion characteristics of molded amorphous boron under different oxygen pressures. *Acta Astronautica*, 138:118-128. https://doi.org/10.1016/j.actaastro.2017.05.019

Liu LL, He GQ, Wang YH, et al., 2015. Chemical analysis of primary combustion products of boron-based fuel-rich propellant. *RSC Advances*, 5(123):101416-101426. https://doi.org/10.1039/C5RA13693H

Liu LL, He GQ, Wang YH, et al., 2017. Factors affecting the primary combustion products of boron-based fuel-rich propellants. *Journal of Propulsion and Power*, 33(2):333-337. https://doi.org/10.2514/1.B36134

Lv Z, Xia ZX, Liu B, et al., 2017. Preliminary experimental study on solid-fuel rocket scramjet combustor. *Journal of Zhejiang University-SCIENCE A (Applied Physics and Engineering)*, 18(2):106-112. https://doi.org/10.1631/jzus.A1600489

Meerov D, Monogarov K, Bragin A, et al., 2015. Boron particles agglomeration and slag formation during combustion of energetic condensed systems. *Physics Procedia*, 72:85-88. https://doi.org/10.1016/j.phpro.2015.09.024

Mi XC, Goroshin S, Higgins AJ, et al., 2013. Dual-stage ignition of boron particle agglomerates. *Combustion and Flame*, 160(11):2608-2618. https://doi.org/10.1016/j.combustflame.2013.06.004

Millot F, Rifflet JC, Sarou-Kanian V, et al., 2002. High-temperature properties of liquid boron from contactless techniques. *International Journal of Thermophysics*, 23(5):1185-1195. https://doi.org/10.1023/A:1019836102776

Roux JA, Choi J, Shakya N, 2014. Parametric scramjet cycle analysis for nonideal mass flow rate. *Journal of Thermophysics and Heat Transfer*, 28(1):166-171. https://doi.org/10.2514/1.T4217

Smolanoff J, Sowa-Resat M, Łapicki A, et al., 1996. Kinetic parameters for heterogenous boron combustion reactions via the Cluster Beam approach. *Combustion and Flame*, 105(1-2):68-79. https://doi.org/10.1016/0010-2180(95)00155-7

Song QG, Cao W, Wei X, et al., 2021. Laser ignition and combustion characteristics of micro- and nano-sized boron under different atmospheres and pressures. *Combustion and Flame*, 230:111420. https://doi.org/10.1016/j.combustflame.2021.111420

Sun YL, Ren H, Du FZ, et al., 2018. Preparation and characterization of sintered B/MgB_2 as heat release material. *Journal of Alloys and Compounds*, 759:100-107. https://doi.org/10.1016/j.jallcom.2018.05.038

Sun YL, Ren H, Jiao QJ, et al., 2020. Oxidation, ignition and combustion behaviors of differently prepared boron-magnesium composites. *Combustion and Flame*, 221:11-19. https://doi.org/10.1016/j.combustflame.2020.07.022

Ulas A, Kuo KK, Gotzmer C, 2001. Ignition and combustion of boron particles in fluorine-containing environments. *Combustion and Flame*, 127(1-2):1935-1957. https://doi.org/10.1016/S0010-2180(01)00299-1

Yetter RA, Rabitz H, Dryer FL, et al., 1991. Kinetics of high-temperature B/O/H/C chemistry. *Combustion and Flame*, 83(1-2):43-62. https://doi.org/10.1016/0010-2180(91)90202-M

Yoshida T, Yuasa S, 2000. Effect of water vapor on ignition and combustion of boron lumps in an oxygen stream. *Proceedings of the Combustion Institute*, 28(2):2735-2741. https://doi.org/10.1016/S0082-0784(00)80694-3

Yuasa S, Isoda H, 1991. Ignition and combustion of small boron lumps in an oxygen stream. *Combustion and Flame*, 86(3):216-222. https://doi.org/10.1016/0010-2180(91)90101-G

Zhang H, Wang NF, Wu ZW, 2020. Effect of fuel grain configuration on the thrust of a solid-fuel scramjet. *Aerospace Science and Technology*, 106:106145. https://doi.org/10.1016/j.ast.2020.106145

Zhou W, 1998. Numerical Study of Multi-Phase Combustion: Ignition and Combustion of an Isolated Boron Particle in Fluorinated Environments. PhD Thesis, Princeton University, Princeton, USA.

Zhou W, Yetter RA, Dryer FL, et al., 1998. Effect of fluorine on the combustion of "clean" surface boron particles. *Combustion and Flame*, 112(4):507-521. https://doi.org/10.1016/S0010-2180(97)00129-6

Zhou W, Yetter RA, Dryer FL, et al., 1999. Multi-phase model for ignition and combustion of boron particles. *Combustion and Flame*, 117(1-2):227-243. https://doi.org/10.1016/S0010-2180(98)00079-0

Electronic supplementary materials

Section S1